# Anisotropic encoding of three-dimensional space by place cells and grid cells

Robin Hayman, Madeleine Verriotis, Aleks Jovalekic, Andre Fenton, Kathryn J. Jeffery

# Anisotropic encoding of three-dimensional space by place cells and grid cells

Hayman, R.[1 *,] Verriotis, M.[1*], Jovalekic, A. [1 *], Fenton, A.A. [2,3], and Jeffery, K.J. [1]

1 Institute of Behavioural Neuroscience
Dept. of Cognitive, Perceptual and Brain Sciences–
Division of Psychology and Language Sciences
University College London
26 Bedford Way
London WC1H 0AP
UK

2 Center for Neural Science
New York University
4 Washington Place
New York, NY 10003

3 Department of Physiology and Pharmacology
State University of New York
450 Clarkson Ave
Brooklyn, NY
New York, NY 11203
USA

[*] These authors contributed equally to the work

Address for correspondence:

Prof. K.J. Jeffery
Institute of Behavioural Neuroscience
Dept. of Cognitive, Perceptual and Brain Sciences
Division of Psychology and Language Sciences
University College London
26 Bedford Way
London WC1H 0AP
Tel: +44 20 7679 5308
Email: k.jeffery@ucl.ac.uk

**The subjective sense of space may result in part from the combined activity of place cells, in the hippocampus, and grid cells in posterior cortical regions such as entorhinal cortex and pre/parasubiculum. In horizontal planar environments, place cells provide focal positional information while grid cells supply odometric (distance-measuring) information. How these cells operate in three dimensions is unknown, even though the real world is three–dimensional. The present study explored this issue in rats exploring two different kinds of apparatus, a climbing wall (the "pegboard") and a helix. Place and grid cell firing fields had normal horizontal characteristics but were elongated vertically, with grid fields forming stripes. It appears that grid cell odometry (and by implication path integration) is impaired/absent in the vertical domain, at least when the animal itself remains horizontal. These findings suggest that the mammalian encoding of three-dimensional space is anisotropic.**

Neural encoding of position is a core cognitive competence depending on activity in a network of structures centred on the hippocampal formation[1]. Hippocampal place cells encode position with localised activity occurring in one or (sometimes) a few locations[2], while neurons upstream, in posterior cortical areas such as entorhinal cortex [3] and pre– and parasubiculum [4], produce extensive evenly spaced firing arrays, called grids, that provide place cells with metric (distance and direction) information. These "grid cells" derive their information, in turn, from a mixture of self-motion cues (path integration) and learned landmarks[5]. Because of their metric properties, grid cells provide an opportunity to elucidate the fundamental metric structure of the mammalian spatial representation (the *cognitive map*[6]).

The properties of the cognitive map on the horizontal plane have been extensively studied, but animals move in three dimensions, and three dimensional movement poses computational challenges not present in two[7]. For example, movement on a slope results in a smaller horizontal translation per unit surface distance covered, and rotations in three dimensions are order-dependent (non-commutative). This raises the question of how the mapping system tracks position for animals moving in non-horizontal environments. Grid cells, because of their odometric properties, offer a unique window into this issue. We show here that place and grid cells exhibit a relative insensitivity to height, with grid cells being even less sensitive than place cells. The cognitive map is thus anisotropic, encoding vertical space differently from horizontal. We suggest that the mammalian cognitive map may be a contextually modulated two-dimensional map rather than a true, volumetric representation.

## RESULTS

We used parametric statistical tests throughout but verified these with more conservative non-parametric tests in cases of skewed distribution; we found no differences between these tests

and so the analyses to follow report the parametric test results. Numbers report mean+/–s.e.m. unless otherwise stated and the results are summarized in Table 1.

In Experiment 1, we recorded place cells from the hippocampal CA1 subfield and grid cells from posterior cortex as rats foraged over a vertically oriented arena having projecting pegs, the pegboard arena (**Fig. 1e**, **Supplementary Fig. 1**). We made comparisons with recordings from horizontal environments.

*Place fields on the vertical arena*

We recorded forty place cells from 7 rats on the pegboard, and compared their firing with 53 cells from 5 rats on a flat arena. Thirty-one cells from 4 rats were recorded in both settings. Place cells fired readily on the pegboard, producing delimited elliptical areas of activity ('place fields'), indicating sensitivity to height as well as horizontal position (**Fig. 1a**; see **Supplementary Fig. 2** for complete data set). Both major and minor axes (length and width, respectively) of the fields were significantly larger on the pegboard (major axes=78+/–3cm on the pegboard and 38+/–2cm on the flat arenas; $t_{(91)}$=11.0, $p<0.0001$; minor axes=39+/–3cm on the pegboard and 21+/–1cm on the flat; $t_{(91)}$=6.1,$p<0.0001$). Place fields on the flat arena were, as is typical of place fields, slightly oval with an aspect ratio of 2.0+/–0.1, consistent with previous measurements[8]. On the pegboard they were more elongated with an aspect ratio of 2.4+/–0.2, significantly greater than that on the flat arenas ($t_{(91)}$=2.2,$p<0.05$; **Fig. 1b**). Because place fields on the pegboard were mostly aligned vertically, by contrast with the horizontal arenas (**Fig. 1c**), it follows that this elongation occurred in the vertical dimension. This was verified by determining the vertical:horizontal span of the fields and comparing this with the ratio obtained by choosing "vertical" and "horizontal" directions on the flat arenas arbitrarily: the difference remained (pegboard ratio=1.8+/–0.1, flat ratio=1.4+/–0.1;$t_{(91)}$=2.6, $p<0.01$).

Spatial information was compared between vertical and horizontal dimensions using Skaggs' method[9], by collapsing the firing rate maps to a linear array either vertically or horizontally (see Supplementary Methods for details). Results are shown in **Fig. 1d**. On the flat arenas the scores for the two dimensions were 0.64+/–0.06 and 0.56+/–0.04 bits for the arbitrary "horizontal" and "vertical", respectively, which did not differ ($t_{(67)}$=1.39, NS). For the pegboard, the horizontal and vertical information scores were 0.66+/–0.06 and 0.24+/–0.02 bits, respectively, which were highly significantly different ($t_{(46)}$=6.86, p<0.001). Thus, place field information content was higher in the horizontal direction than the vertical for the vertical arena (the pegboard).

To assess place field modulation by height, the pegboard was binned into 5 horizontal layers (**Fig. 1e**) and firing rates (% peak) calculated for each cell on each layer: 19/40 fields spanned all 5 layers and 21/40 spanned <5 layers (**Fig. 1f**). The fields, despite their elongation, were somewhat height-modulated, since even when the peak layer was excluded, intensity of individual fields fell steadily with increasing distance from the peak rather than simply fluctuating (**Supplementary Fig. 3**; R=–0.55, p<0.0001).

*Grid fields on the vertical arena*

We recorded seventeen grid cells from 5 rats on the pegboard, and compared their firing with 34 cells from 10 rats on a flat arena. Sixteen cells from 5 rats were recorded in both settings (**Fig 2a**, see **Supplementary Fig. 4** for the complete data set). The cells produced grid-like periodic firing on the flat arenas (**Fig. 2a**, **Supplementary Fig. 4a–d**). They also fired on the vertical pegboard, but strikingly, instead of producing vertical grids they produced vertically aligned stripes (**Fig. 2**, **Supplementary Fig. 4e–h**). This elongation of the firing fields was reflected in their size and aspect ratio characteristics (Table 1): major axes averaged 98+/–4cm on the pegboard compared with 52+/–5cm on the flat arenas ($t_{(38)}$=6.7, p<0.0001). By

contrast, minor axes did not differ, being 38+/–3cm on the pegboard and 35+/–4cm on the flat ($t_{(38)}$=0.5,NS), resulting in a significantly increased aspect ratio on the pegboard (3.0+/–0.4) compared with the flat (1.5+/–0.1; $t_{(38)}$=4.6, p<0.0001; **Fig. 2b**). As with the place cells, most of this difference could be accounted for by vertical stretching (**Fig. 2c**): the vertical:horizontal size ratio was 2.3+/–0.2 on the pegboard and (arbitrarily chosen) "vertical":"horizontal" on the flat was significantly less, at 1.2+/–0.1 ($t_{(38)}$=4.7, p<0.0001). An ANOVA comparing the aspect ratios for 17 grid fields and 17 randomly selected place fields from the pegboard and flat conditions revealed no effect of cell type [$F_{(1,64)}$=0.5, NS] but a main effect of environment [$F_{(1,64)}$=11, p<0.01] and a significant cell x environment interaction [$F_{(1,64)}$=5.3, p<0.05]. Post-hoc pairwise analyses (Tukey's) revealed that grid fields were significantly narrower than place fields on the flat ($t_{(32)}$=2.41, p<0.05) but not on the pegboard ($t_{(32)}$=1.58, NS). The vertical field size count showed that of the 17 grid fields, 13 spanned all 5 layers and only 4 spanned <5 layers (**Fig. 2e**). The elongation was significantly greater for grid cells than place cells (Chi-square test of 5 layers vs fewer for place and grid cells: $\chi^2(1, N=57)=4.07$, p<0.05; **Fig. 2f**).

As with the place cells, grid field spatial information content was calculated for each dimension separately (**Fig. 2d**). On the flat arenas the (arbitrarily chosen) "horizontal" and "vertical" information scores were 0.29+/–0.04 and 0.25+/–0.03 bits, respectively, which did not differ ($t_{(33)}$=1.3,NS). For the pegboard, the horizontal and vertical information scores were 0.55+/–0.06 and 0.17+/–0.03 bits, respectively, which differed significantly ($t_{(16)}$=6.2, p<0.0001). Thus, information content for grid cells was much lower in the vertical dimension on the vertical arena. Comparison of vertical information for grid cells and place cells on the pegboard found no difference ($t_{(62)}$=1.6, NS). A symmetry analysis (see Supplementary Methods for details) found that grid cell firing fields had six-fold symmetry on the flat and two-fold symmetry on the pegboard (**Supplementary Fig. 5**).

The stripes resulted from the vertical orientation of the pegboard, because on the same apparatus laid horizontally, grid cells produced grids (**Supplementary Fig. 6**). To additionally rule out locomotor confounds we classified the spike data from the pegboard trials according to whether the rat was moving up, down, left or right: stripes persisted in all travel directions (**Supplementary Fig. 7**).

We next looked to see whether stripe spacing was similar to the spacing of the same cell's fields on a flat arena (**Supplementary Fig. 8**). For the 16 cells recorded on both arenas, we compared stripe width and spacing on the pegboard with that on the flat arenas. Stripe width averaged 37+/–2cm and subfield width did not differ at 31+/–7cm ($t_{(24)}$=0.64, NS): nor did these values correlate (R=0.39, NS). However, subfield spacing and stripe spacing values, which were also similar (68+/–4cm and 66+/–3cm, respectively; t(24)=0.38, NS), did correlate (R=0.71, $p<0.05$). One cell expressed three stripes for which the inter-stripe spacings were, interestingly, unequal, consistent with the stripes being randomly oriented cross-sections through a hexagonal-columnar array of firing fields (**Fig. 5C**).

Although the firing fields appeared as stripes, the vertical rate analysis found, as for place cells, a decline across layers (**Supplementary Fig. 3**; R=–0.59, $p<0.0001$), indicating some rate modulation by height, suggesting that either the stripes are actually long thin ovals, or else there is some thinning of the fields, perhaps due to edge effects, at the top and bottom borders of the apparatus.

The observations on the pegboard were made on a two-dimensional environment. In Experiment 2, we made recordings on a helical track (**Fig. 3b**, **Supplementary Fig. 1b**), which allows animals to move in three dimensions, albeit with yoking of horizontal and vertical displacements. Rats shuttled between the top and bottom of the transparent helix several times per session, circumnavigating five (4 hippocampal and 6 entorhinal rats) or six

(2 hippocampal rats) coils. Horizontal position was recorded by an overhead camera that could see the head-mounted LED through the Plexiglas, and vertical position was derived by counting the number of coils circumnavigated. For position analyses, we compared the real place and grid cells against "dummy" cells, constructed by selecting a field for each coil at random from the complete data set, to abolish between-coil correlations. We compared data from the helix with data from the flat environments from Experiment 1.

*Place fields on the helix*

For the purposes of description, a "run" is an excursion from top to bottom, and a coil is a circumnavigation, which could occur at any level (**Supplementary Fig. 9**). Separate analyses were run for each direction but as the results were similar a combined analysis is reported throughout. Analyses for the 5-coil and 6-coil version of the helix are combined unless stated otherwise.

Seen from above, with all the coils collapsed together, place cells produced spatially localized fields (**Fig. 3a**, left plots). To determine the dimensional characteristics of the firing fields, each coil of the helix was unwound to produce a linear 64-bin plot of position (**Supplementary Fig. 9**). Place cells usually fired differently on up/clockwise vs. down/counter-clockwise runs, with 92% being strongly modulated in rate, position or both. Therefore, we treated upwards and downwards runs as different data sets.

Place cell firing recurred on multiple coils (**Fig. 3a**; see **Supplementary Fig. 10** for the complete data set). The firing locations on the different coils were highly correlated ($R=0.500$), by contrast with the control set of dummy place cells ($R=0.005$; $Z_{(N=151)}=9.9$, $p<0.0005$; Mann-Whitney test), and only small lateral shifts of the coils (4.6 bins) compared with the dummy cells (16.3 bins; $Z_{(N=191)}=9.8$, $p<0.0005$; Mann-Whitney) were required to maximise the between-coils correlation (**Fig. 3c**): firing thus recurred at the same relative

location and did not "remap" between coils. Henceforth, fields were treated as unitary, vertical ellipses, with height being the major axis and extent along the track the minor axis.

The axis dimensions, and aspect ratios, of the firing fields are shown in **Fig. 3d** and summarized in **Table 1**. The minor axis averaged 40+/–2cm, larger than the minor axis on the flat (21+/–1 cm; $t_{(150)}$=5.44, p<0.0001) but similar to the 38+/–2cm long major axis of place fields on the flat arenas ($t_{(87)}$=0.5, NS). Vertical field extent averaged 69+/–2cm, which was significantly greater than the horizontal dimension (40+/–2cm; $t_{(204)}$=11.8, p<0.0001). It was, however, less than the major axis of place fields on the pegboard (78+/–3cm; $t_{(141)}$=2.6, p<0.01), perhaps because the helix was less tall. The aspect ratio for place fields on the helix was 2.1+/–0.1, similar to that on the flat arenas (2.0 +/– 0.1; $t_{(154)}$=1.00, NS) but less than that on the pegboard (2.4 +/– 0.2; $t_{(91)}$=2.16, p<0.05). Fields on the 5-coil helix tended to be smaller than on the 6-coil helix in both horizontal extent (35+/–3cm and 45+/–4cm, respectively; $t_{(101)}$=2.2, p<0.05) and vertical extent (63+/–2cm and 75+/–2cm respectively; $t_{(101)}$=4.3, p<0.0001), and thus did not differ in their aspect ratios (2.2+/–0.1 and 2.1+/–0.1 respectively; $t_{(101)}$=0.4, NS).

The vertical distribution of place field peaks is shown in **Fig. 3e**. Although there were slightly more at the top and bottom, this distribution did not differ from uniform ($\chi^2$ (2, *N*=215)=5.1, NS). Cells with differing vertical spreads were counted as for the pegboard, using coils instead of layers. While 32 fields spanned all 5 coils, only 18 spanned fewer (**Fig. 3f** and **Supplementary Fig. 11**). Thus, as on the pegboard, fields on the helix tended to occupy a long vertical extent, but not always. Despite the elongation of the fields, place cell firing rates as a function of distance from the peak steadily attenuated (**Supplementary Fig. 3**; R=–0.36, $t_{(462)}$=8.25, p<0.0001), unlike dummy place cell firing rates (R=–0.032, $t_{(406)}$ = 0.64, p>0.05).

In sum, place cells appeared to be somewhat modulated by vertical travel distance on the

helix, as they were on the pegboard.

*Grid fields on the helix*

Grid cell firing patterns, when viewed from above, similarly resembled those seen in the open-field arena: that is, with typically more than one activity peak (**Fig. 4a**; see **Supplementary Fig. 12** for the complete data set). Like place cells, grid cells were frequently modulated by direction of run (**Fig. 4b**), and so we again analysed up-going and down-going runs separately, and compared real data with dummy data.

Position analysis confirmed that firing recurred at the same place on each coil (correlations R=0.63 and R=–0.01 for grid cells and dummy grid cells, respectively, $Z_{(N=105)}$=8.6, p<0.0005; lateral shifts=3.9 and 16.7 bins for grid cells and dummy cells, respectively, $Z_{(N=105)}$=8.1, p<0.0005; both Mann-Whitney; **Fig. 4c**). The horizontal extent of grid fields along the track (minor axis) averaged 28+/–2cm, which was not different from the minor axis on the flat (35+/–4cm; $t_{(74)}$=1.6, NS; **Fig. 4d** and **Table 1**). The inter-peak distance between fields on the track ranged from 19–66cm (mean+/–s.e.m.=44+/–2cm). Vertical field extent averaged 69+/–1cm, which was greater than the horizontal dimension ($t_{(104)}$=17.6, p<0.0001) and greater than the major axis of fields on the flat ($t_{(74)}$=5.1, p<0.0001). Like the place fields, this was, however, less than the vertical extent of grid fields on the pegboard (98+/–4cm; $t_{(68)}$=7.82, p<0.0005). The aspect ratio was 2.9+/–0.1 overall, which – by contrast with the place fields – was significantly different from that on the flat arenas (1.5+/–0.1; $t_{(74)}$=6.33, p<0.0001) and indistinguishable from that on the pegboard (3.0+/–4; $t_{(68)}$=0.0, NS). An ANOVA comparing aspect ratios on the flat arenas vs. the helix for 23 grid fields and 23 randomly chosen place fields (92 fields altogether), found a main effect of cell type [$F_{(1,88)}$=6.6, p<0.05], a main effect of environment [$F_{(1,88)}$=23.6, p<0.001] and a significant interaction [$F_{(1,88)}$=26,1, p<0.001]. Post hoc pairwise comparisons (Tukey's) found that place field aspect ratios did not

differ between flat arenas and helix (ratios both 1.9) but grid fields differed significantly (ratios of 1.5+/–0.3 on the flat and 2.9+/–1.0 on the helix; $t_{(44)}$=6.66, p<0.0001). Furthermore, on the helix, grid field aspect ratios were significantly greater than those of place fields ($t_{(44)}$=4.27, p<0.0001). Thus, grid fields were more elongated than place fields on the helix.

The vertical distribution of grid field peaks is shown in **Fig. 4e** and **Supplementary Fig. 11**. As with place fields, there were slightly more at the top and bottom but not significantly ($\chi^2$ (2, *N*=121)=0.82, NS). We counted the numbers of fields with different coil spans, as for place cells. By contrast with the place cells, grid cells were more inclined to fire on all coils, and firing very rarely if ever fell to zero on any coil (**Fig. 4f**, **Supplementary Fig. 12**). Thus, of the 53 primary grid fields, 44 fired on all 5 coils, while only 7 fired on 4 coils and 2 on 3 coils. A Chi-square analysis comparing fields spanning 5 vs. less than 5 coils between place and primary grid cells found a significant difference ($\chi^2$(1, *N* =103)= 4.81, p < 0.05). Thus, while place cells showed a degree of modulation by height, grid cells showed less. Nevertheless, grid cell firing rates did also fall away progressively from the peak (**Supplementary Fig. 3**; R=–0.30, $t_{(314)}$ = 5.54, p<0.0001), unlike dummy grid firing rates (R=0.022, $t_{(206)}$ = 0.32, p>0.05).

## DISCUSSION

Our study shows that place and grid cells showed less sensitivity to height than to horizontal displacement, and it thus appears that “neural odometry” was selectively impaired in the vertical dimension. Most notably, grid cells, which show periodic firing in the horizontal plane, showed no vertical periodicity. The similarity of results from environments of differing structure and which elicited different locomotor behaviour suggests that the neural representation of allocentric space has intrinsically different properties in the vertical dimension from those in the horizontal, and is therefore anisotropic.

Although both place and grid fields were vertically elongated, they were nevertheless somewhat height-modulated on both apparati, with place cells – interestingly – being more modulated than grid cells. This modulation suggests that height *is* encoded by these cells, but in a different way. The difference may be merely one of scale – had we used very tall environments, we might have seen grids occurring over a very large scale, producing apparent stripes on a small apparatus but revealing periodicity on a large one (**Fig. 5a**). However, it may be that the difference is qualitative rather than quantitative: the *way* in which firing is modulated differs in vertical vs. horizontal dimensions. Place fields have been shown to respond to qualitative as well as quantitative variations in environmental stimuli, as evidenced by their altered firing in response to changes in "context" (reviewed in [10]). Given that changes in an animal's height produce changes in qualitative contextual aspects of the environment, over and above mere metric changes in height, it may be that these are what modulate firing in the vertical dimension. Such contextual modulation could explain why there is a dissociation between the sensitivity of grid cells and place cells to height: possibly place cells are informed about height, via their contextual inputs, in a way that grid cells are not.

There have been earlier suggestions that encoding of the vertical dimensions may be non-metric in place cells. Initial studies of place cells on a sloping or vertically translated surface found evidence of sensitivity to vertical displacement[11-13] and also to tilt[13] but little evidence of true metric encoding. However, this could have been due to the strong salience of local cues conferred by the environment surfaces, causing odometry to be dominated by the floor. On our pegboard apparatus, by contrast, the wall provided the dominant (and indeed, only) surface: odometry was preserved in the horizontal dimension, despite the absence of a horizontal surface, but impaired in the vertical dimension despite the vertical surface. Thus, the impaired vertical odometry does not seem to be due to the surface structure of the environment.

The pattern of grid cell stripes on the pegboard is consistent with the stripes being cross sections through a hexagonal close-packed columnar array (**Fig. 5b**) which could explain the irregular inter-stripe spacing (**Fig. 5c**). However, the stripes are also reminiscent of the findings of Derdikman et al. [14] of directionally dependent stripe-like activity on a hairpin maze composed of repeating segments. Instead of a continuous pattern of grid fields, the grid cell responses in the maze repeated on each successive entry into identical maze sub-compartments, introducing a discontinuity in the grid pattern that apparently indicated failure of the cells to take into account (i.e., path integrate) distance travelled in the direction orthogonal to the linear compartments. Notably, cells were highly directional in this apparatus, suggesting that the two opposing directions of travel were treated as different environments, or "contexts". However, fields on the pegboard were not directional, and nor did rats execute such stereotyped movements that their trajectories could be broken up into compartment-like blocks. Furthermore, on the helix, unlike the discontinuous grid pattern in the hairpin maze, we observed a continuous, repeating pattern of grid bumps. The differences occurring between our experiments and that of Derdikman et al. suggests that the phenomena may be different. However, the common feature of pattern repetition seen in these environments may reflect the common feature of impaired path integration in the direction orthogonal to the main direction of travel.

The results on the helix similarly resemble those of Nitz[15] who found that place field patterns repeated on successive laps of a horizontal spiral. The cells failed to encode the lateral translation that occurred with each successive lap of the spiral, in a manner analogous to how our cells failed to encode the vertical translation that occurred on each lap. This suggests a general hypothesis: that path integration does not function effectively for movement in a dimension that is perpendicular to the long axis of the animal (which usually includes, for surface-dwelling animals, the vertical dimension). An analogous finding has been reported in

head direction cells, which encode directions only in the plane of locomotion [16], apparently producing a planar compass signal, but one that can be oriented vertically if the animal – unlike on our pegboard – orients its body plane vertically.

Impaired vertical odometry might result from the fact that there is less visual information about vertical travel. We think it unlikely that vertical cues are more impoverished, as the experimental rooms possessed many features at multiple vertical levels (shelves, doors etc; **Supplementary Fig. 1**), and in any case, in the horizontal plane, place and grid fields are usually well formed even when the only source of visual discontinuity is a cue card. We therefore suggest that impaired vertical path integration is the likelier explanation. Models of grid cell generation postulate a metric process by which interfield spacing is computed[17-19]: like the metric models of place field generation, these models could account for the vertical elongation by presuming a deficient or absent distance-calculating process for travel in the direction perpendicular to the animal's head/body plane.

The generality of the present findings is a question for future research. In both apparati, rats travelled on a surface and it may be that this impaired the ability of the allocentric spatial system to form a volumetric representation. Alternatively, since rats are surface-travelling it may be that the system has, in rats and other surface-travelling species, lost some of its ability to represent space volumetrically (that is, with metric information in all three dimensions), even in a volumetric environment. However, it is also possible that the planar character of the cognitive map is a general feature of animals in all settings. Representing three dimensions volumetrically is computationally highly complex, partly because it requires many more representational units (scaling as the square of the equivalent horizontal component), and also – more importantly – because it requires an integrated 3D compass having four degrees of freedom (three for heading – one in each rotational plane – plus one for orientation of the head/body around the long axis), for which there is no evidence in any animal at present. As

humans, our subjective sense of 3D space feels integrated and three-dimensional. However, experiments in zero gravity where subjects can move freely in all directions find that they nevertheless tend to impose a reference "horizontal" on the environment[20]. This suggests that our own internal representation of space may also be planar, and that our sense of having a complete 3D spatial map may be an illusion. This has important consequences for understanding human exploration and mapping of 3D spaces such as undersea, air, space and – more recently – virtual reality.

## METHODS

*Subjects and apparatus*

We implanted rats with tetrodes aimed at dorsal CA1 (n=12), dorsomedial mEC (n=9) or postsubiculum (n=1; this was from another experiment, but yielded a grid cell which may have been a perforant path fiber from the dentate molecular layer [21]. All procedures were performed under UK Home Office licence authority according to the Animals (Scientific Procedures) Act 1986.

The pegboard (**Fig. 1e**, **Supplementary Fig. 1a**) comprised a vertically oriented wooden board 121x121 cm square, studded at 10–20 cm intervals with projecting wooden dowels (17cm x 9 mm). The helical track (**Fig. 3b**, **Supplementary Fig. 1b**) comprised Perspex triangular steps anchored at the innermost end and winding in a right-handed spiral around a central core, making five or six complete turns, each of pitch 14.4 cm. The helix was 52 cm in diameter and the central core was 33 cm in diameter. A horizontally aligned camera viewed the pegboard, and a downwards-pointing ceiling-mounted camera viewed the helix. Control environments were square or circular arenas 60–200 cm across.

*Electrode implantation and recording*

Recording electrodes were four moveable tetrodes aimed at hippocampus (co-ordinates –3.8–4.0 mm AP, 2.2–2.5 mm ML, 1.5 mm DV), dMEC (tetrodes angled 6–10 degrees in the parasagittal plane and implanted at 0.1–0.3 mm anterior to the transverse sinus, 4.0–4.5 mm ML, and 1.5–2.0 mm DV) or postsubiculum (AP –6.7 mm, ML 2.8 mm, DV 1.6 mm).

After recovery, recordings were made using an Axona DacqUSB system. Once place or grid cells were isolated, we placed the animals on one of the environments to explore for food while spike data were collected. On the pegboard, rats foraged by clambering over the pegs (**Fig. 1**) for 10–30 minutes. On the helical track, rats repeatedly ran from the bottom to the top and back again, with reward at both ends. Trials consisted of 20 minutes or 14 runs, whichever was shorter.

*Data analysis*

We isolated units using a cluster cutting program (Tint, Axona Ltd). Cells were considered place units if their activity occurred on electrodes in the hippocampus, had a peak rate > 1 Hz, totalled > 50 spikes and showed, on the open field or pegboard, spatially localised firing (coherence value >0.66) or showed, on the helical track, firing on more than one run. We considered cells to be probable grid cells if their activity occurred on electrodes aimed at entorhinal cortex, had a peak rate > 1 Hz, and had localised firing in at least one location that remained stable in at least one environment.

We constructed position-normalised firing rate maps as described in the SOM, defining the field containing the peak firing as the “main field”. For open field and pegboard analyses, we used smoothed rate maps to derive field length and width, aspect ratio, orientation and – for grid cells – inter-peak spacing (for multiple fields) and symmetry order.

*Pegboard analysis*

Because the constrained trajectories on the pegboard caused firing field fragmentation, we implemented an algorithm to coalesce these (see SOM for details). A similar procedure was applied to control data except for grids with small spacing and multiple fields, which would be spuriously coalesced. We used the major and minor axes of the resulting fields to derive aspect ratio and major-axis orientation of the main fields. For grid cells, we generated two-dimensional autocorrelation maps [3, 22]. Skaggs' spatial information[9] was calculated for the two-dimensional maps. Then, we extracted one-dimensional subcomponents by collapsing and averaging the smoothed firing rate maps first horizontally, and then vertically.

For vertical rate analysis, we binned the pegboard data into five horizontal layers, thus matching the helical track, and compared the numbers of fields spanning all 5 layers vs 1–4 layers between place and grid fields. To determine whether firing was smoothly height-modulated or fluctuated randomly, regression analysis compared firing rate (% peak rate) against distance (in layers) from the peak (excluding the peak itself).

We calculated stripe width and stripe spacing on the pegboard for grid cells by collapsing the smoothed data into one row of firing rates, and counting bins with firing above 15% peak rate in order to derive stripe width. We applied a similar procedure to the best grid field from a trial recorded in a horizontal arena. Where possible, we calculated inter-stripe spacing using a linear spatial autocorrelation.

*Helical track analysis*

We decomposed the helical track data into individual coils which we then linearized. (**Supplementary Fig. 9**) and divided into 64 bins. From this, we calculated position-normalised firing rate. The resulting maps were boxcar-smoothed (width = 5). A field

comprised regions of at least 5 consecutive bins with firing greater than 15% peak rate. We compared real data against a control "dummy" data set constructed from actual fields randomly chosen from the complete set.

We next examined horizontal and vertical field properties. Horizontally, two measures examined whether fields recurred in the same horizontal co-ordinates on different coils. First, we computed pairwise between-coil bin-for-bin Pearson's R correlations. Second, for each pair of coils we calculated the relative offset (measured in bins, with wraparound at the coil ends) that would maximise this correlation. To obtain horizontal field size, we collapsed the helix by averaging the rates for each bin across all coils, smoothing as above and counting bins with firing above 15% peak rate. For grid cells with multiple fields we averaged this value. Grid field spacing was determined from a linear spatial autocorrelation.

Vertical field analysis determined the vertical location of field peaks, vertical extent of fields and vertical aspect ratio. To determine whether firing was smoothly height-modulated or fluctuated randomly, we used a regression analysis to compare firing rate (% peak rate) against distance in coils from the peak (excluding the peak itself).

## ACKNOWLEDGEMENTS

The work was supported by grants from the Wellcome Trust and the European Commission Framework 7 ("Spacebrain") to KJ, and a National Science Foundation grant to AAF. We thank Eduard Kelemen for help designing and Mark Shkop for constructing the helical track, Emma Leeper for building the pegboard arena, Menno Witter for advice on histology and Caswell Barry and Francesca Cacucci for comments on the manuscript.

## AUTHOR CONTRIBUTIONS

RH, MV and AJ contributed equally to the work. RH and MV implanted animals, recorded and analysed the bulk of the data and wrote most of the methods and supplementary methods. AJ recorded the bulk of the pegboard data and contributed analysis and methods. AF conceived the helical track, oversaw its construction and advised on data analysis and interpretation. KJ conceived and gained funding for the overall research programme, designed the pegboard and oversaw its construction, supervised the data collection and analysis and wrote the introduction and discussion.

## COMPETING FINANCIAL INTERESTS

The authors have no competing financial interests.

## TABLE LEGEND

Comparison of firing field characteristics for place and grid cells on apparati of differing form and dimensionality.

## FIGURE LEGENDS

**Figure 1** Place fields on the pegboard. (a) Firing fields of 10 hippocampal place cells recorded in 60cm square horizontal environments and on the 1.2 m square vertical pegboard. Each field is shown as raw data (black traces = rat's path, blue squares = superimposed action potentials) and as smoothed contour plots with peak rate (Hz) in white text. Colour bar shows percentages of peak firing. (b) Length (mean +/– s.e.m.) of the major (long) and minor (short) axes, and aspect ratios (mean +/– s.e.m.), of fields in the flat arenas and pegboard. F = Flat, PB = pegboard. * = $p < 0.05$, *** = $p < 0.0001$. (c) Orientations of place fields in the two environments. In the flat arenas (light blue), 90 degrees was arbitrarily aligned with one pair

of arena walls. Place field orientation showed two peaks (asterisks) at 90 and 180 degrees, reflecting the tendency of place fields to align with walls. On the pegboard (dark blue), almost all fields aligned vertically (90 degrees). (d) One-dimensional spatial information content (mean +/– s.e.m.) for firing rate maps collapsed horizontally (H) or vertically (V), in either flat arenas (H and V arbitrarily chosen) or on the pegboard, showing significantly less information in the vertical dimension on the pegboard. (e) Diagram of the pegboard, showing the analysis layers (labelled according to a hypothetical cell with field peak in the central layer). (f) Percentages of firing fields having different vertical extents (specified as layer span).

**Figure 2** Grid fields on the pegboard. (a) Firing fields of 12 grid cells on the flat arenas (left plots) and on the vertical pegboard (right plots). Fields are as described in **Fig. 1a** except that spikes are red. In the flat environments, firing fields were multiple and arranged approximately in a hexagonal close-packed array. On the pegboard, by contrast, the fields tended to be aligned in one or more vertical stripes. Peak rates (Hz) in white text. Colour bar shows percentages of peak firing. (b) Field sizes and aspect ratios (mean +/– s.e.m.). On the pegboard, and by contrast with the place cells (**Fig. 1b**), the major axis increased in size whereas the minor axis did not, with a consequent increase in aspect ratio. (c) Orientation of the grid fields, illustrated as in **Fig. 1c**. (d) Spatial information content (mean +/– s.e.m.) as shown in **Fig. 1d**. (e) Percentages of firing fields having different vertical extents (specified as layer span). (f) Comparison of number of place and grid fields spanning all 5 layers vs. fewer (* = $p < 0.05$).

**Figure 3** Place fields on the helix. (a) Firing patterns of 8 place cells on the track, as seen from overhead (left and middle, details as in **Fig. 1b**) or decomposed into firing rate histograms from individual coils (right). Data represent up- or down-going runs, but not both. Peak rates (Hz) are shown in black text for the overhead rate maps. Colour bar shows

percentages of peak firing. (b) Schematic of the helical track. (c) Between-coil field correlation (median +/– quartiles) for place fields vs. dummy place fields (left) and lateral shift (median +/– quartiles) that maximised between-coil correlations for place fields and dummy place fields (right). (d) Major (long or vertical) and minor (short or horizontal) field axes (left), and aspect ratios (right), for place fields on the helix vs. the flat environments (mean +/– s.e.m.). F = Flat, Hx = Helix. (e) Distribution of place field peaks across the vertical extent of the helix. (f) Comparison of place field size for the five-coil and six-coil configurations of the track.

**Figure 4** Grid fields on the helix. (a) Firing patterns of 8 grid cells on the helix, (details as in **Fig. 3a** but with spikes in red). Peak rates (Hz) are shown in black text for the overhead rate maps. Colour bar shows percentages of peak firing. (b) Grid cell coil-by-coil rate histograms, showing up-going and down-going runs separately, for 4 cells that showed significant directional modulation. (c) Between-coil field correlation (median +/– quartiles) for grid fields vs. dummy grid fields (left) and lateral shift (median +/– quartiles) that maximised between-coil correlations for grid fields and dummy grid fields (right), decomposed into up-going (. (d) Major (long or vertical) and minor (short or horizontal) field axes (left), and aspect ratios (right), for grid fields on the helix vs. the flat environments (mean +/– s.e.m.). F = Flat, Hx = Helix. (e) Distribution of grid field peaks across the vertical extent of the helix. (f) Vertical field size comparison for place vs. grid cells, showing increased tendency for grid cells to have fields that span the entire vertical extent of the helix.

**Figure 5** Hypotheses concerning the firing patterns observed in the present experiment. (a and b) Two hypotheses about why grid fields appear vertically elongated on the pegboard. (a) The stripes could result from vertical stretching of an intrinsically hexagonal field array (shown for arrays at two different orientations) which is then sampled by the pegboard (squares). (b) The stripes could result from transection of an intrinsically columnar field array.

(c) Observation of a cell with variable inter-stripe spacing favors the columnar-transection hypothesis (see text for details). (d) Schematic of the hypothesis that the repeating fields across coils represent successive transections of an intrinsically columnar firing field by the helix.

## REFERENCES


1. Burgess, N. Spatial cognition and the brain. *Ann. N. Y. Acad. Sci.* **1124**, 77-97 (2008).

2. Moser, E.I., Kropff, E., & Moser, M.B. Place cells, grid cells, and the brain's spatial representation system. *Annu. Rev. Neurosci.* **31**, 69-89 (2008).

3. Hafting, T., Fyhn, M., Molden, S., Moser, M.B., & Moser, E.I. Microstructure of a spatial map in the entorhinal cortex. *Nature* **436**, 801-806 (2005).

4. Boccara, C.N. *et al.* Grid cells in pre- and parasubiculum. *Nat. Neurosci.* **13**, 987-994 (2010).

5. Barry, C., Hayman, R., Burgess, N., & Jeffery, K.J. Experience-dependent rescaling of entorhinal grids. *Nat. Neurosci* **10**, 682-684 (2007).

6. O'Keefe,J. & Nadel,L. *The Hippocampus as a Cognitive Map* (Clarendon Press, Oxford, 1978).

7. Jeffery,K. Navigating in a 3D world in *Animal Thinking: Contemporary Issues in Comparative Cognition* (The MIT Press, 2011).

8. Hartley, T., Burgess, N., Lever, C., Cacucci, F., & O'Keefe, J. Modeling place fields in terms of the cortical inputs to the hippocampus. *Hippocampus* **10**, 369-379 (2000).

9. Skaggs, W.E., ., M.B.L., Gothard, K.M., & Markus, E.J. An information-theoretic approach to deciphering the hippocampal code. *Adv. Neural Inf. Process Syst.* **5**, 1031-1037 (1993).

10. Jeffery, K.J. Integration of the sensory inputs to place cells: what, where, why, and how? *Hippocampus* **17**, 775-785 (2007).

11. Knierim, J.J. & McNaughton, B.L. Hippocampal place-cell firing during movement in three-dimensional space. *J. Neurophysiol.* **85**, 105-116 (2001).

12. Knierim, J.J., McNaughton, B.L., & Poe, G.R. Three-dimensional spatial selectivity of hippocampal neurons during space flight. *Nat. Neurosci* **3**, 209-210

(2000).

13. Jeffery, K.J., Anand, R.L., & Anderson, M.I. A role for terrain slope in orienting hippocampal place fields. *Exp. Brain Res.* **169**, 218-225 (2006).

14. Derdikman, D. *et al.* Fragmentation of grid cell maps in a multicompartment environment. *Nat. Neurosci.* **12**, 1325-1332 (2009).

15. Nitz, D.A. Path shape impacts the extent of CA1 pattern recurrence both within and across environments. *J. Neurophysiol.*(2011).

16. Stackman, R.W., Tullman, M.L., & Taube, J.S. Maintenance of rat head direction cell firing during locomotion in the vertical plane. *J. Neurophysiol.* **83**, 393-405 (2000).

17. McNaughton, B.L., Battaglia, F.P., Jensen, O., Moser, E.I., & Moser, M.B. Path integration and the neural basis of the 'cognitive map'. *Nat. Rev. Neurosci* **7**, 663-678 (2006).

18. O'Keefe, J. & Burgess, N. Dual phase and rate coding in hippocampal place cells: theoretical significance and relationship to entorhinal grid cells. *Hippocampus* **15**, 853-866 (2005).

19. Fuhs, M.C. & Touretzky, D.S. A spin glass model of path integration in rat medial entorhinal cortex. *J Neurosci* **26**, 4266-4276 (2006).

20. Tafforin, C. & Campan, R. Ethological experiments on human orientation behavior within a three-dimensional space--in microgravity. *Adv. Space Res.* **14**, 415-418 (1994).

21. Leutgeb, J.K., Leutgeb, S., Moser, M.B., & Moser, E.I. Pattern separation in the dentate gyrus and CA3 of the hippocampus. *Science* **315**, 961-966 (2007).

22. Sargolini, F. *et al.* Conjunctive representation of position, direction, and velocity in entorhinal cortex. *Science* **312**, 758-762 (2006).

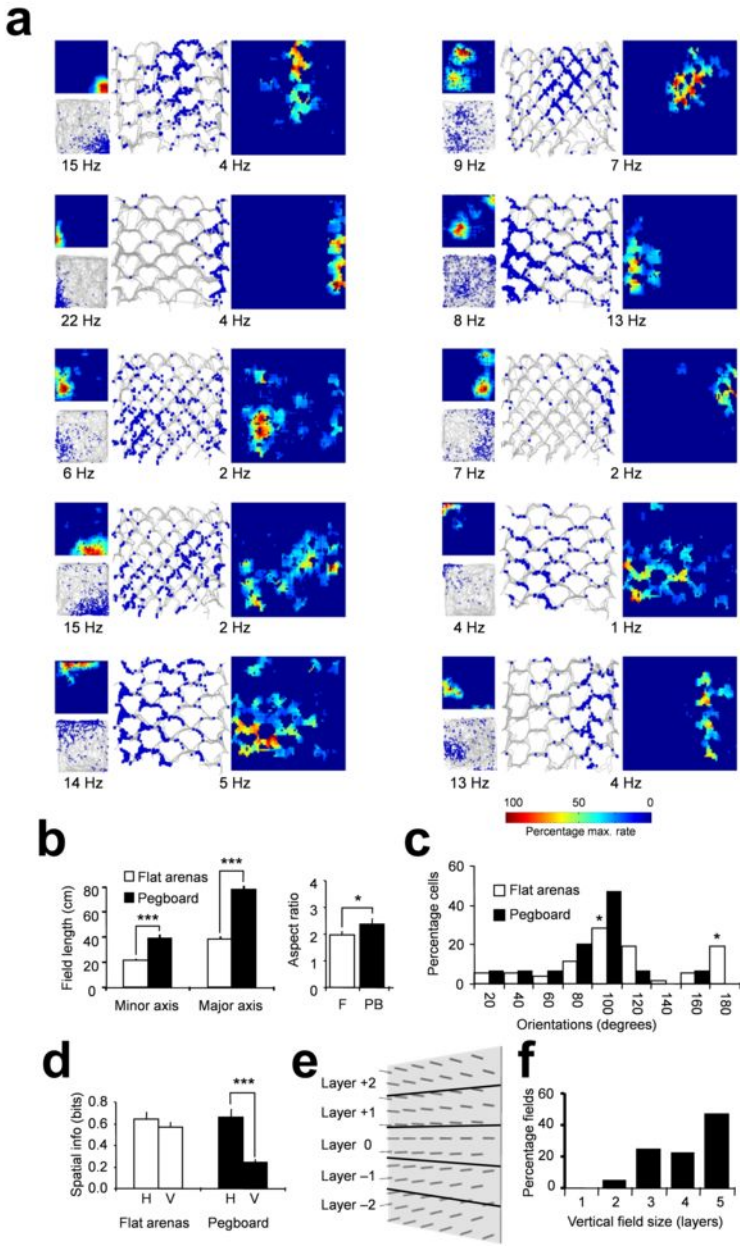
a
15 Hz
4 Hz
9 Hz
7 Hz
22 Hz
4 Hz
8 Hz
13 Hz
6 Hz
2 Hz
7 Hz
2 Hz
15 Hz
2 Hz
4 Hz
1 Hz
14 Hz
5 Hz
13 Hz
4 Hz
100
50
0
Percentage max. rate
b
Flat arenas
Pegboard
Field length (cm)
***
***
Minor axis
Major axis
Aspect ratio
*
F
PB
c
Flat arenas
Pegboard
Percentage cells
*
*
Orientations (degrees)
d
Spatial info (bits)
***
H
V
H
V
Flat arenas
Pegboard
e
Layer +2
Layer +1
Layer 0
Layer –1
Layer –2
f
Percentage fields
Vertical field size (layers)

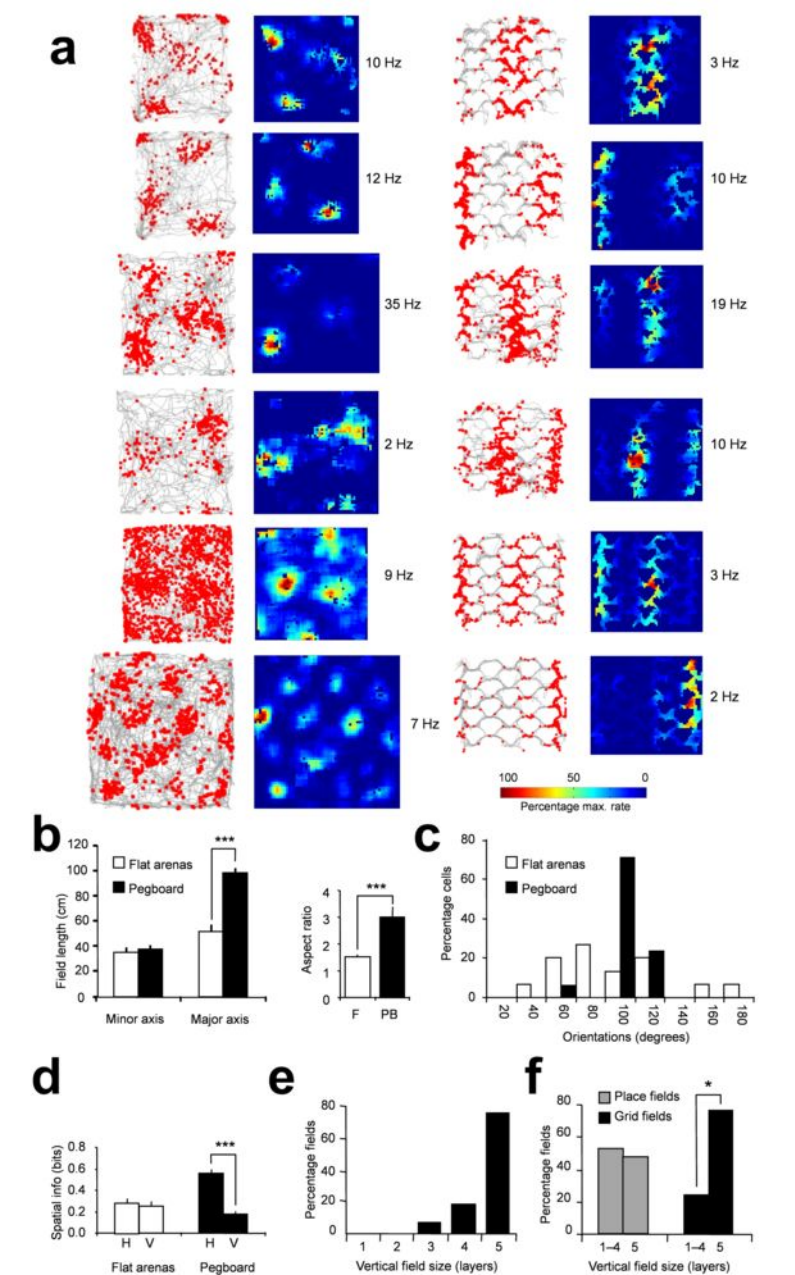
a
10 Hz
12 Hz
35 Hz
2 Hz
9 Hz
7 Hz
3 Hz
10 Hz
19 Hz
10 Hz
3 Hz
2 Hz
100
50
0
Percentage max. rate
b
Flat arenas
Pegboard
Field length (cm)
***
Minor axis
Major axis
Aspect ratio
***
F
PB
c
Flat arenas
Pegboard
Percentage cells
Orientations (degrees)
d
Spatial info (bits)
***
H
V
H
V
Flat arenas
Pegboard
e
Percentage fields
Vertical field size (layers)
f
Place fields
Grid fields
Percentage fields
*
1–4
5
1–4
5
Vertical field size (layers)

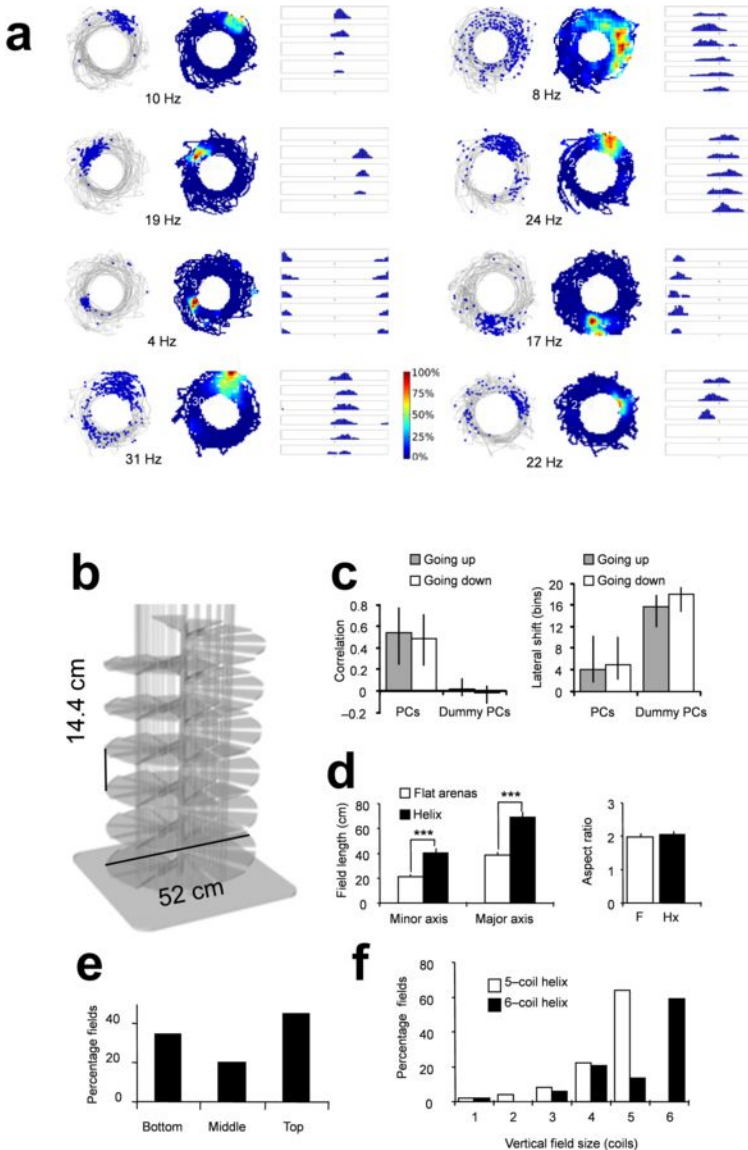
a
10 Hz
8 Hz
19 Hz
24 Hz
4 Hz
17 Hz
31 Hz
22 Hz
100%
75%
50%
25%
0%
b
14.4 cm
52 cm
c
Going up
Going down
Correlation
PCs
Dummy PCs
Lateral shift (bins)
d
Flat arenas
Helix
Field length (cm)
Minor axis
Major axis
Aspect ratio
F
Hx
e
Percentage fields
Bottom
Middle
Top
f
5–coil helix
6–coil helix
Percentage fields
Vertical field size (coils)

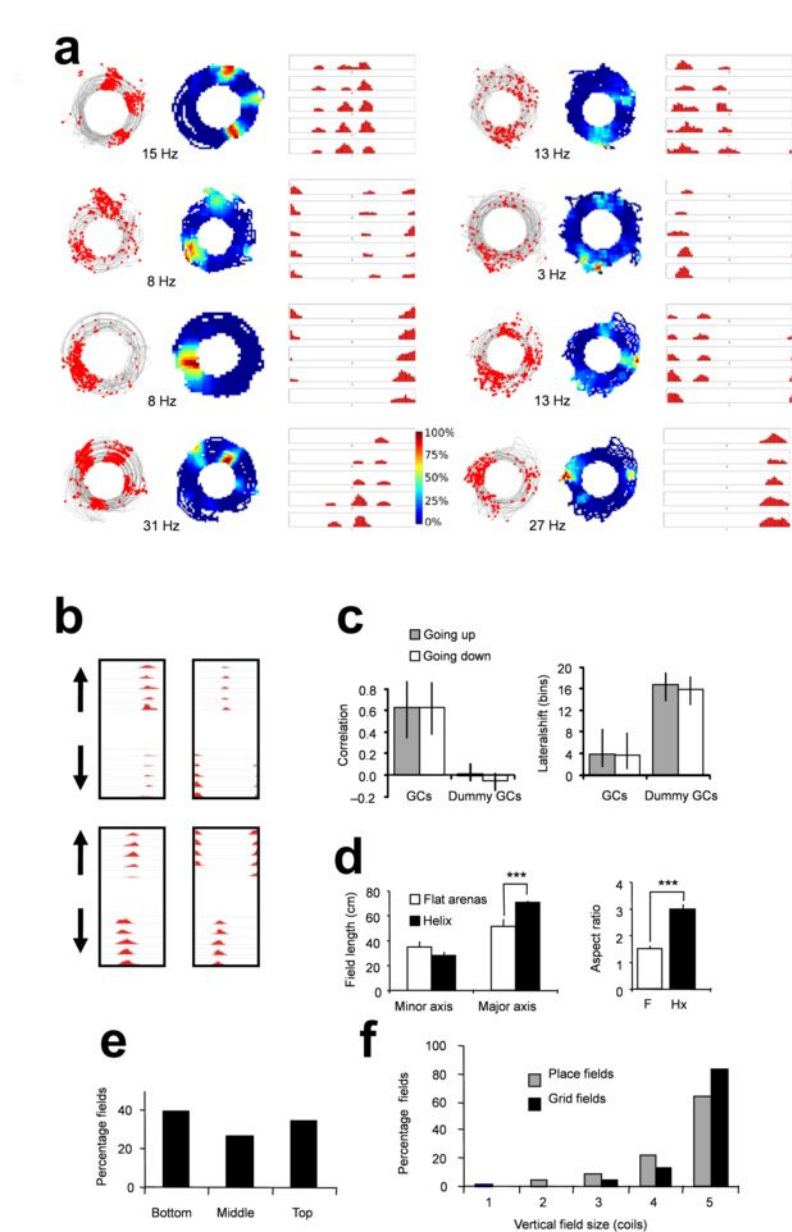
a
15 Hz
13 Hz
8 Hz
3 Hz
8 Hz
13 Hz
31 Hz
27 Hz
100%
75%
50%
25%
0%
b
c
Going up
Going down
Correlation
0.8
0.6
0.4
0.2
0.0
−0.2
GCs
Dummy GCs
Lateralshift (bins)
20
16
12
8
4
0
GCs
Dummy GCs
d
Flat arenas
Helix
Field length (cm)
80
60
40
20
0
***
Minor axis
Major axis
Aspect ratio
4
3
2
1
0
***
F
Hx
e
Percentage fields
40
20
0
Bottom
Middle
Top
f
Percentage fields
100
80
60
40
20
0
Place fields
Grid fields
1
2
3
4
5
Vertical field size (coils)

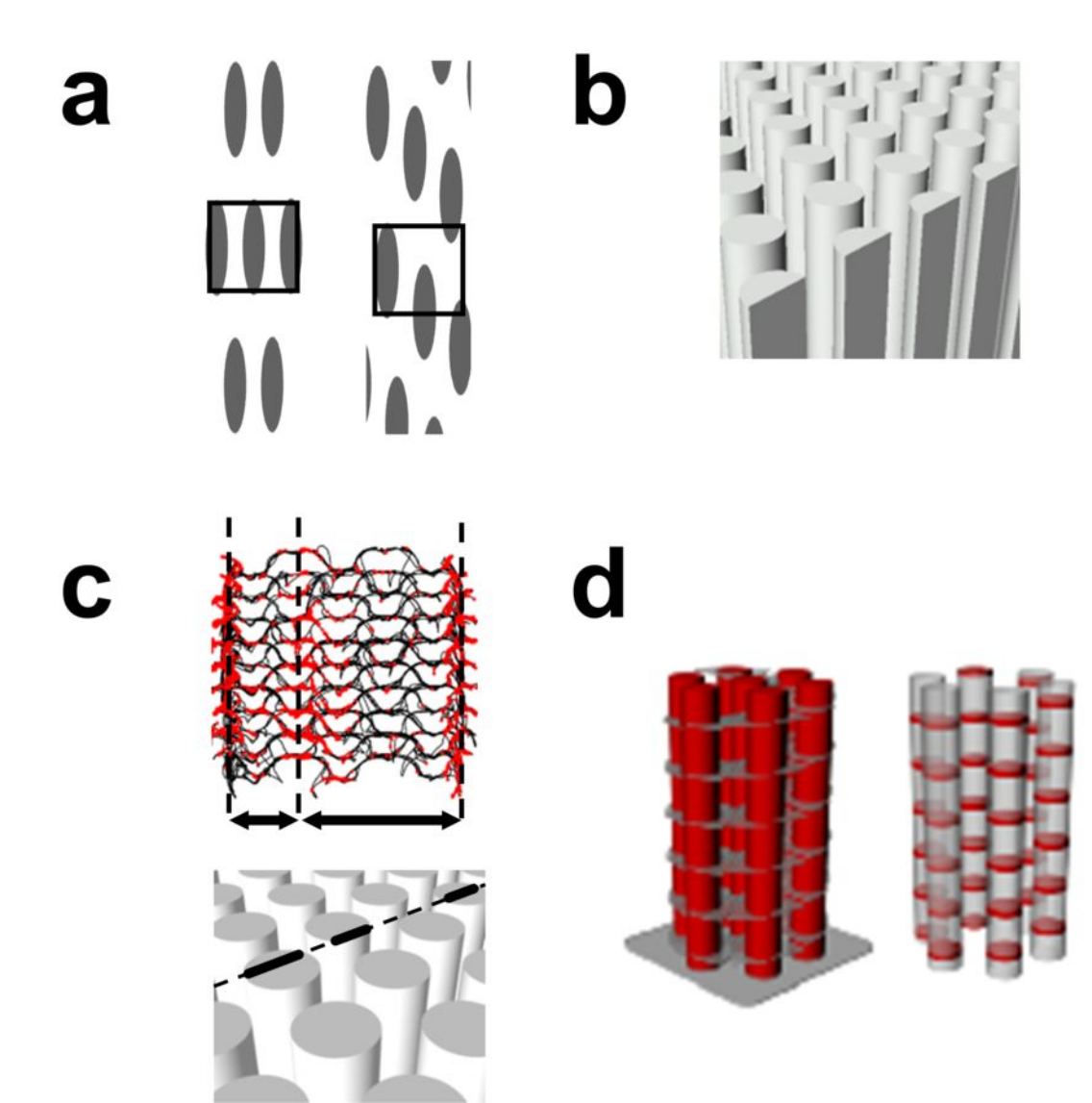
a
b
c
d

**Table 1**

Comparison of firing field characteristics for place and grid cells on apparati of differing form and dimensionality.

| | | Place fields | | | Grid fields | | |
|---|---|---|---|---|---|---|---|
| | | n | Mean | s.e.m | n | Mean | s.e.m |
| **Peak firing rate (Hz)** | Flat arenas | 53 | 9.8 | 0.9 | 23 | 7.8 | 1.4 |
| | Pegboard | 40 | 5.1 | 0.5 | 17 | 5.6 | 1.3 |
| | Helix | 103 | 10.3 | 0.7 | 53 | 9.5 | 1.0 |
| **Major axis/height (cm)** | Flat arenas | 53 | 38 | 2 | 23 | 52 | 5 |
| | Pegboard | 40 | 78 | 3 | 17 | 98 | 4 |
| | Helix (5-coil) | 50 | 63 | 2 | 53 | 69 | 1 |
| | Helix (6-coil) | 53 | 75 | 2 | - | - | - |
| | Helix (all) | 103 | 69 | 2 | 53 | 69 | 1 |
| **Minor axis/ width (cm)** | Flat arenas | 53 | 21 | 1 | 23 | 35 | 4 |
| | Pegboard | 40 | 39 | 3 | 17 | 38 | 3 |
| | Helix (5-coil) | 50 | 35 | 3 | 53 | 28 | 2 |
| | Helix (6-coil) | 53 | 45 | 4 | - | - | - |
| | Helix (all) | 103 | 40 | 2 | 53 | 28 | 2 |
| **Aspect ratio** | Flat arenas | 53 | 2.0 | 0.1 | 23 | 1.5 | 0.1 |
| | Pegboard | 40 | 2.4 | 0.2 | 17 | 3.0 | 0.4 |
| | Helix (5-coil) | 50 | 2.2 | 0.1 | 53 | 2.9 | 0.1 |
| | Helix (6-coil) | 53 | 2.1 | 0.1 | - | - | - |
| | Helix (all) | 103 | 2.1 | 0.1 | 53 | 2.9 | 0.1 |
| **Skaggs info (total bits/spike)** | Flat arenas | 53 | 1.63 | 0.10 | 23 | 1.00 | 0.09 |
| | Pegboard | 40 | 1.16 | 0.10 | 17 | 0.77 | 0.07 |
| **Skaggs info (horiz. bits/spike)** | Flat arenas | 53 | 0.66 | 0.07 | 23 | 0.29 | 0.04 |
| | Pegboard | 40 | 0.66 | 0.09 | 17 | 0.55 | 0.06 |
| **Skaggs info (vert. bits/spike)** | Flat arenas | 53 | 0.58 | 0.05 | 23 | 0.25 | 0.03 |
| | Pegboard | 40 | 0.29 | 0.03 | 17 | 0.17 | 0.03 |